

Supporting Information

Catalyst-Derived Hierarchy in 2D Imine-Based Covalent Organic Frameworks

Hao Guo¹, Joseph P. Cline², Ryan Thorpe³, Christopher J. Kiely^{1,2,3},
Srinivas Rangarajan¹, Mark A. Snyder^{1*}

¹ Dept. of Chemical and Biomolecular Engineering, Lehigh University, Bethlehem, PA 18015,
United States

² Dept. of Materials Science and Engineering, Lehigh University, Bethlehem, PA 18015,
United States

³ Institute for Functional Materials and Devices, Lehigh University, Bethlehem, PA 18015,
United States

* Corresponding author: snyder@lehigh.edu (M.A. Snyder)

Contents

1. Morphology of COFs synthesized with different amounts of acetic acid and a low concentration of 0.002 eq. Sc(OTf) ₃	2
2. Reproducibility of COFs synthesized under different catalytic conditions and different reaction times.....	3
3. FTIR spectra of as-made COFs, monomers, solvents, and Sc(OTf) ₃ catalyst.....	6
4. Sc(OTf) ₃ dispersion in COF-LZU1 particles.....	6
5. XPS-based elemental analysis of as-made COFs.....	7
6. Crystallographic analysis of as-made COFs: Reaction time sensitivity, indexing, analysis and estimation of edge amine content.....	11
7. DFT simulation of metal triflate binding to COF framework functionality as a function of metal	16
8. Evolution of the morphology, composition, and crystallinity of as-made COF-LZU1 under 0.02 eq. Sc(OTf) ₃ with different amounts of DI water	16
9. COF-LZU morphology upon activation.....	17
10. Theoretical pore size changes with defect introduction.....	18
11. Hierarchical COF Literature comparison	18
12. RdB and MB adsorption equilibration times.....	19
13. References.....	19

1. Morphology of COFs synthesized with different amounts of acetic acid and a low concentration of 0.002 eq. $\text{Sc}(\text{OTf})_3$

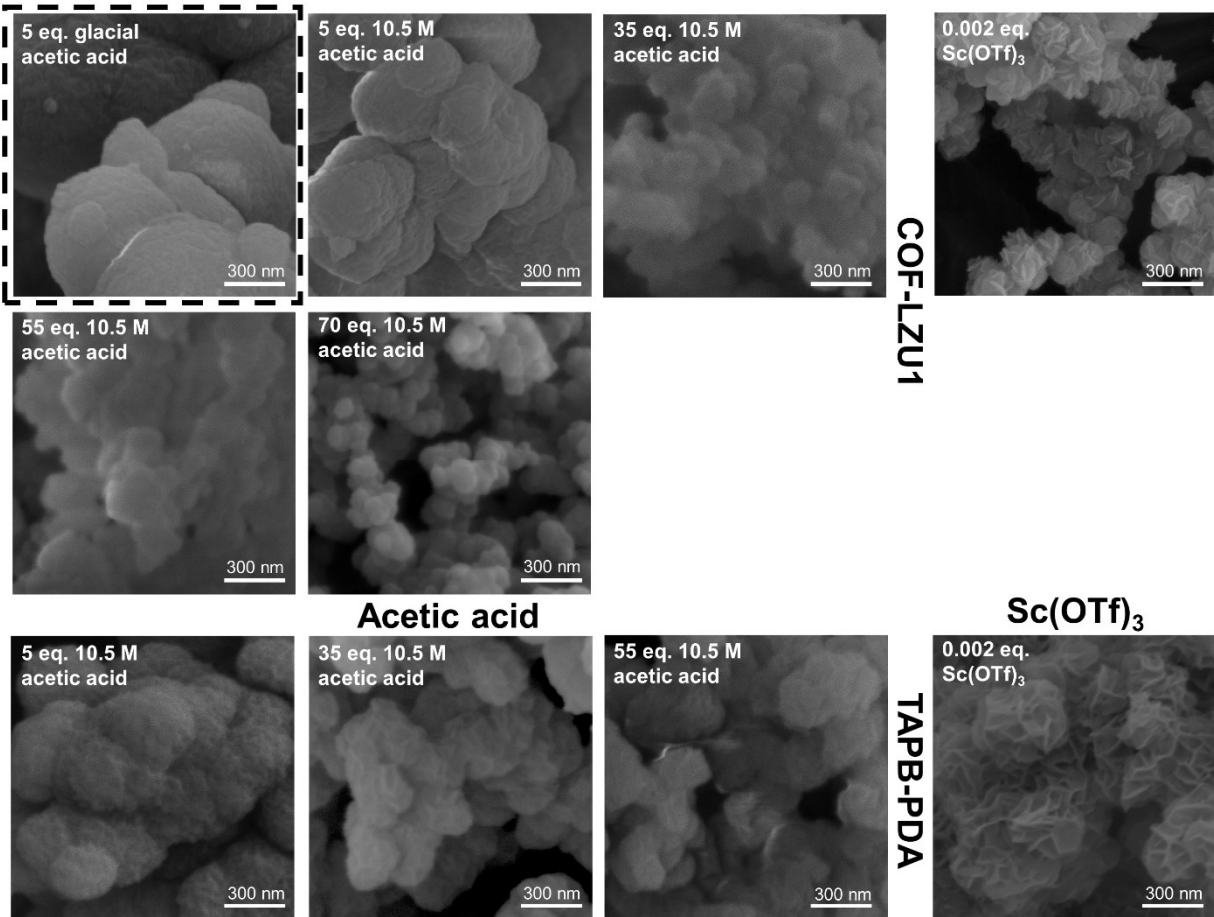


Figure S1. SEM images of as-made COF-LZU1 and TAPB-PDA synthesized under different catalytic conditions.

2. Reproducibility of COFs synthesized under different catalytic conditions and different reaction times

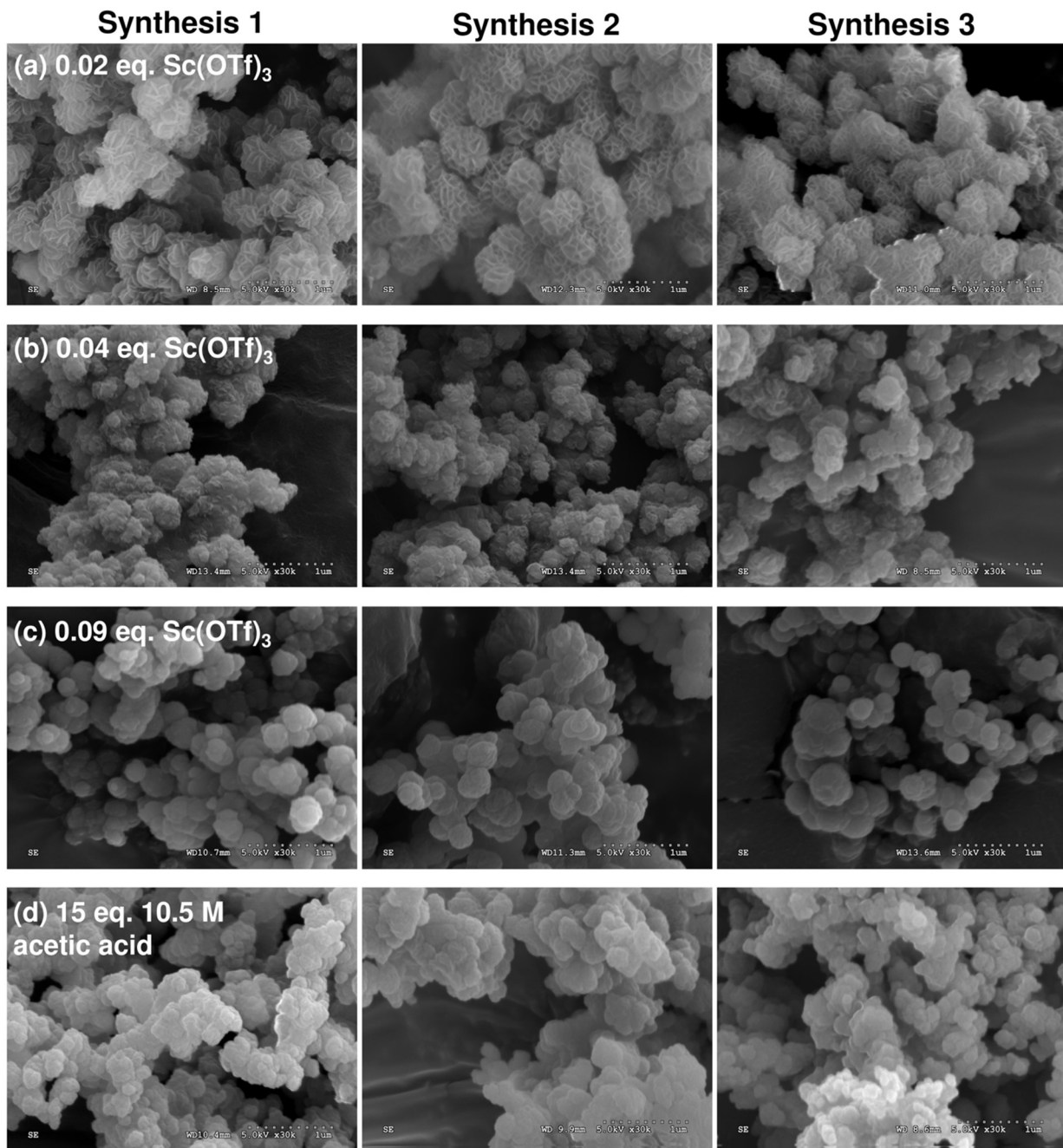


Figure S2. SEM images of COF-LZU1 synthesized under different catalytic conditions (rows) and in different batches (columns) with a reaction time of 1 h.

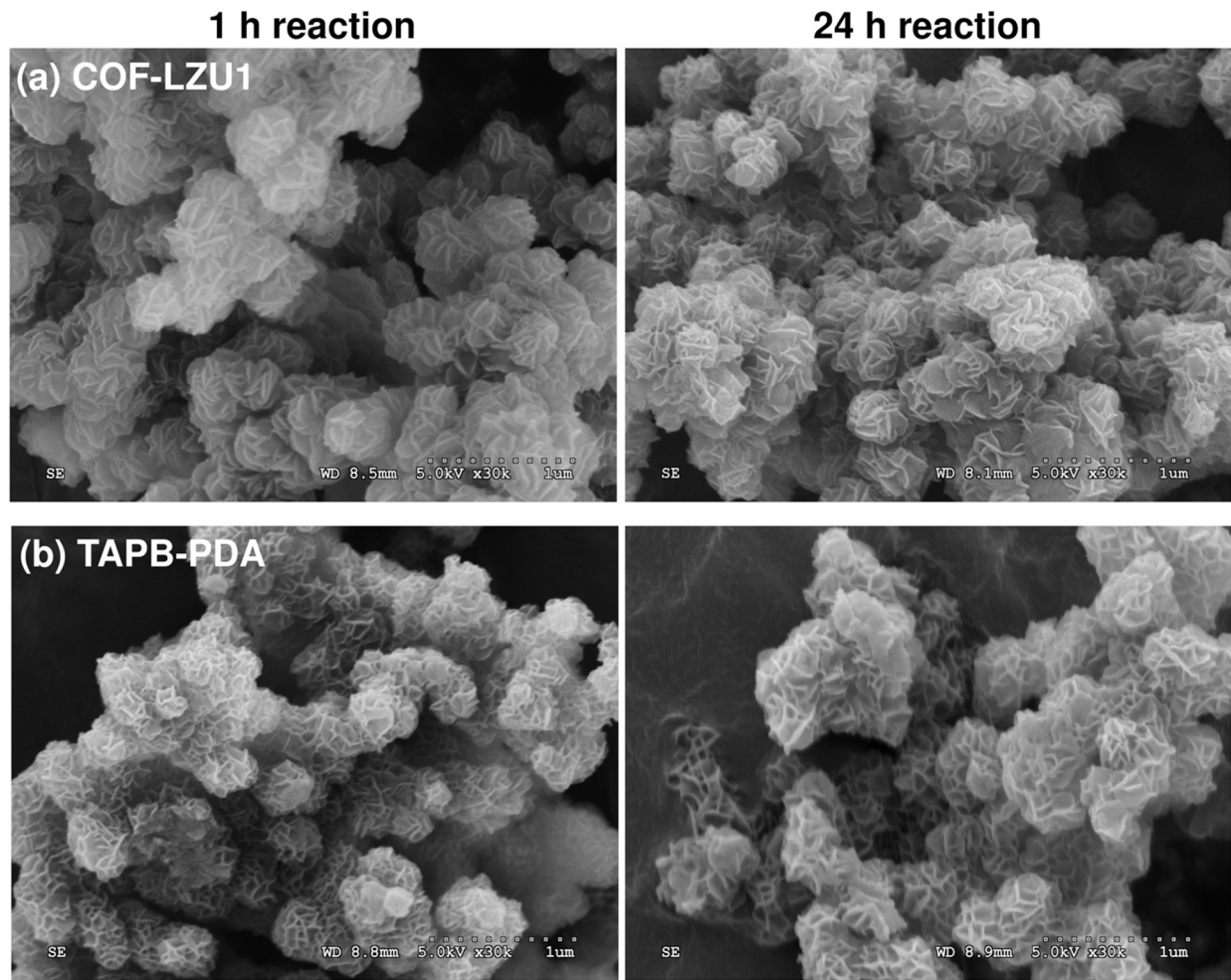


Figure S3. SEM images of as-made COF-LZU1 and TAPB-PDA synthesized under 1 h and 24 h reactions catalyzed by 0.02 eq. $\text{Sc}(\text{OTf})_3$.

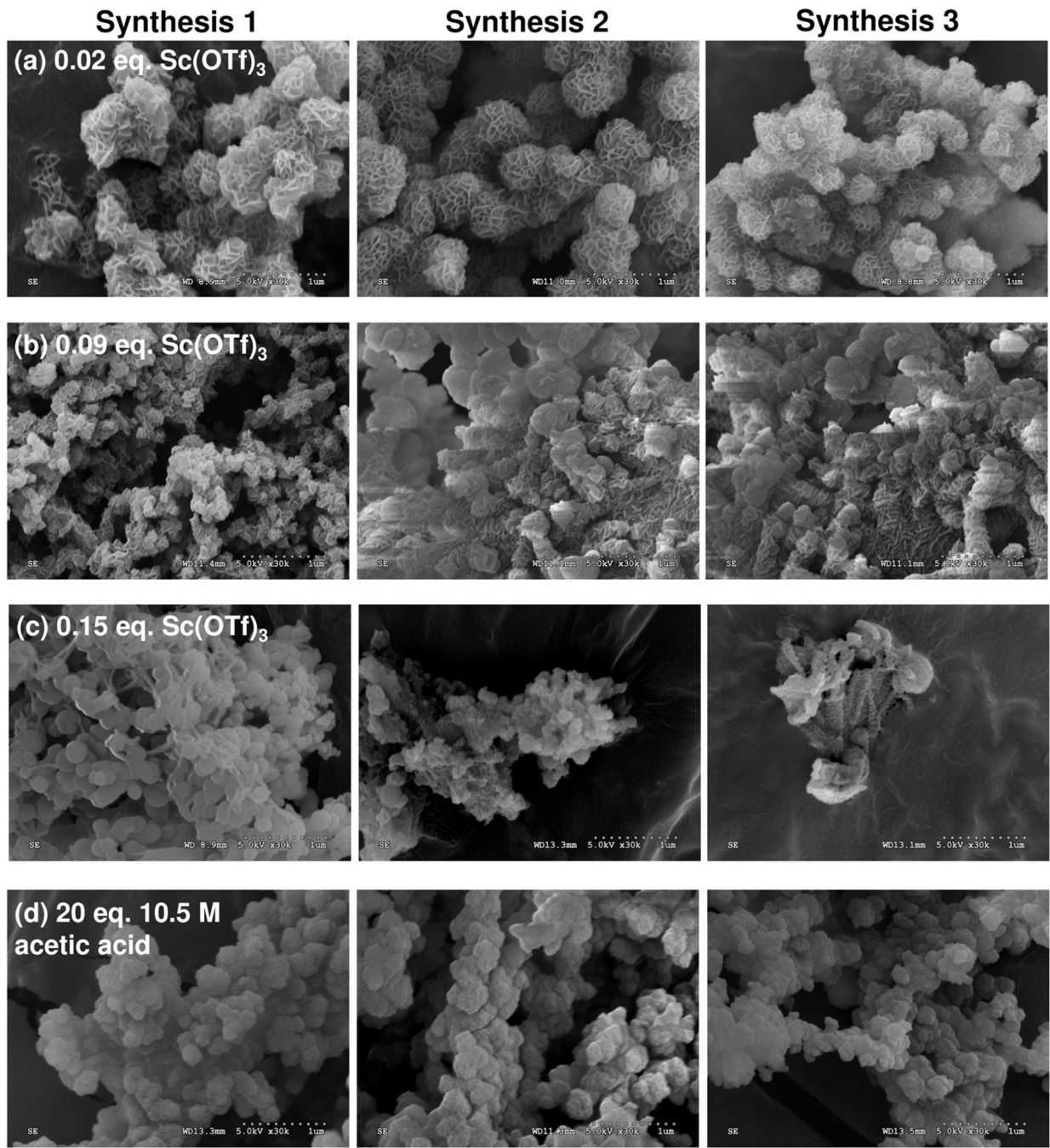


Figure S4. SEM images of TAPB-PDA synthesized under different catalytic conditions (rows) and in different batches (columns) with a reaction time of 24 h.

3. FTIR spectra of as-made COFs, monomers, solvents, and $\text{Sc}(\text{OTf})_3$ catalyst

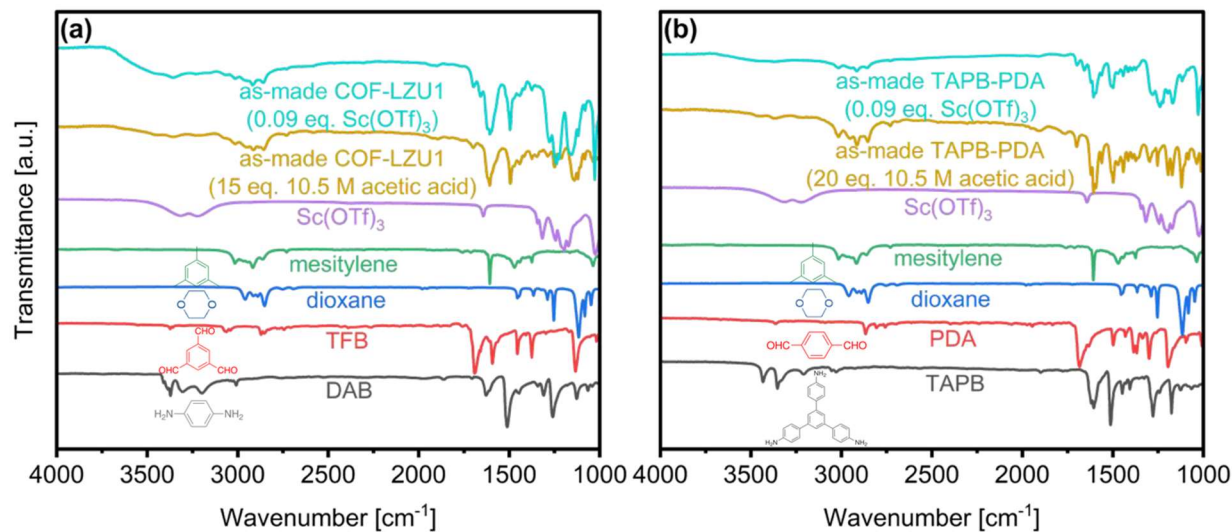


Figure S5. FTIR spectra of monomers, reaction solvents, $\text{Sc}(\text{OTf})_3$, and as-made (a) COF-LZU1 and (b) TAPB-PDA synthesized under different catalytic conditions.

4. $\text{Sc}(\text{OTf})_3$ dispersion in COF-LZU1 particles

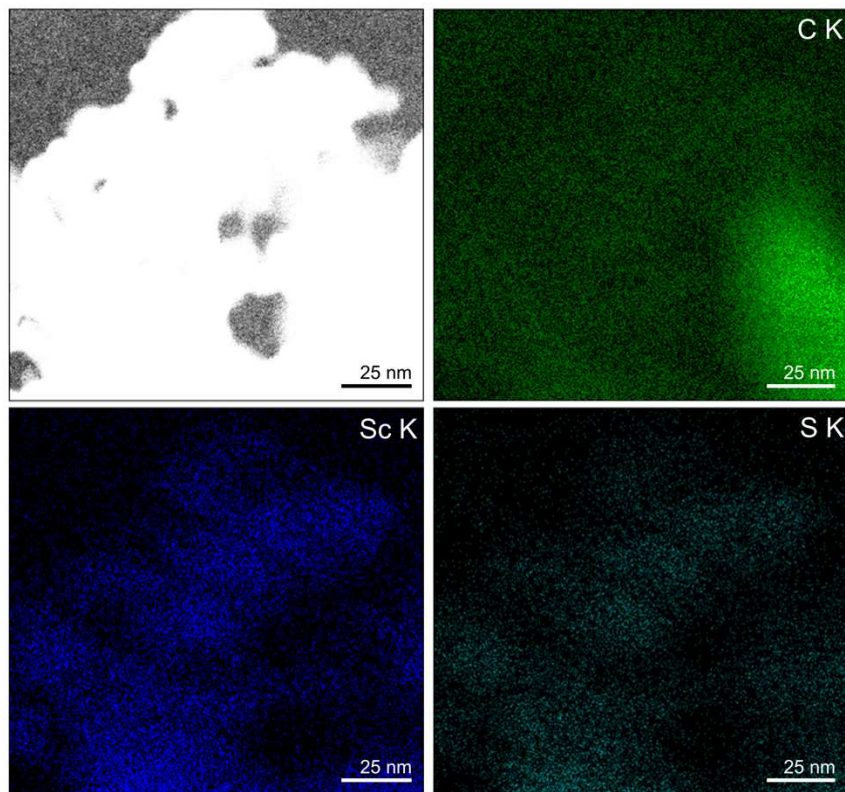


Figure S6. EDS elemental mapping of as-made COF-LZU1 synthesized under 0.02 eq. $\text{Sc}(\text{OTf})_3$.

5. XPS-based elemental analysis of as-made COFs

XPS analysis: XPS peak fitting and assignments were carried out according to literature references¹⁻³ and published elemental spectra (<https://www.thermofisher.com/us/en/home/materials-science/learning-center/periodic-table.html>) according to areas of fitted peak associated with (a) the 1s orbital for C, N, O, and F, and (b) the 2p_{3/2} peak from the 2p orbital of Sc and S, normalized by the sensitivity factor of the element orbital. The atom % is calculated as the normalized area of a specific peak divided by the sum of normalized areas of representative peaks for all atoms. Atom percentages computed for the pristine COFs accounted for contributions from Sc(OTf)₃.

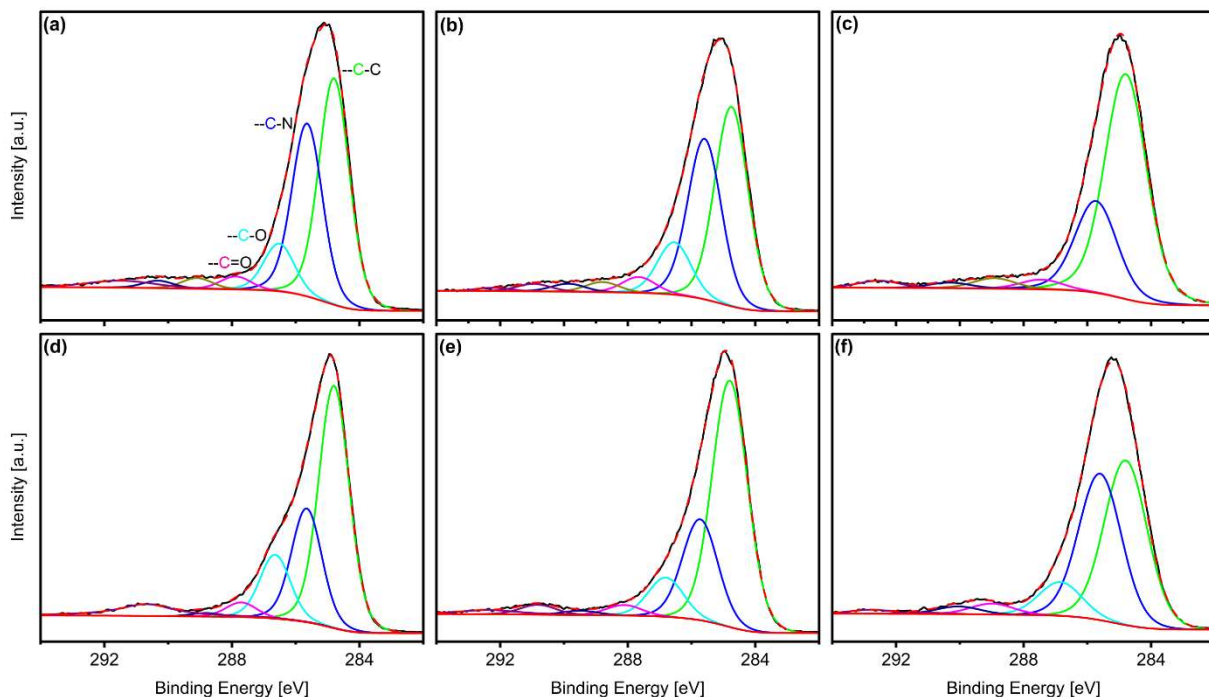


Figure S7. C 1s XPS spectra for as-made COF-LZU1 synthesized under (a) 15 eq. 10.5 M acetic acid, (b) 0.02 eq. Sc(OTf)₃, and (c) 0.09 eq. Sc(OTf)₃, and as-made TAPB-PDA synthesized under (d) 15 eq. 10.5 M acetic acid (e) 0.02 eq. Sc(OTf)₃ (f) 0.15 eq. Sc(OTf)₃.

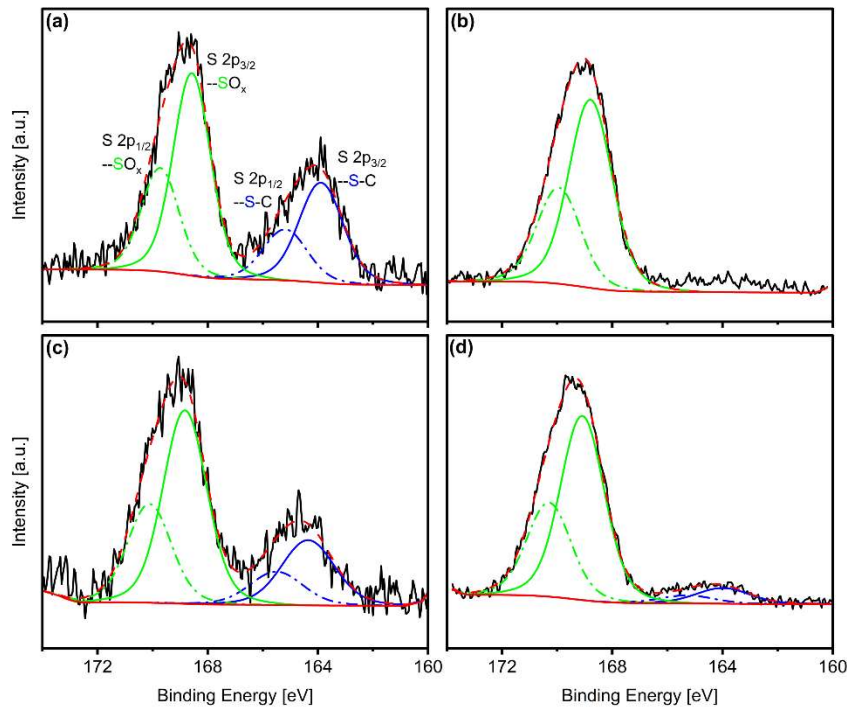


Figure S8. S 2p XPS spectra for as-made COF-LZU1 synthesized under (a) 0.02 eq. Sc(OTf)₃ and (b) 0.09 eq. Sc(OTf)₃, and as-made TAPB-PDA synthesized under (c) 0.02 eq. Sc(OTf)₃ and (d) 0.15 eq. Sc(OTf)₃.

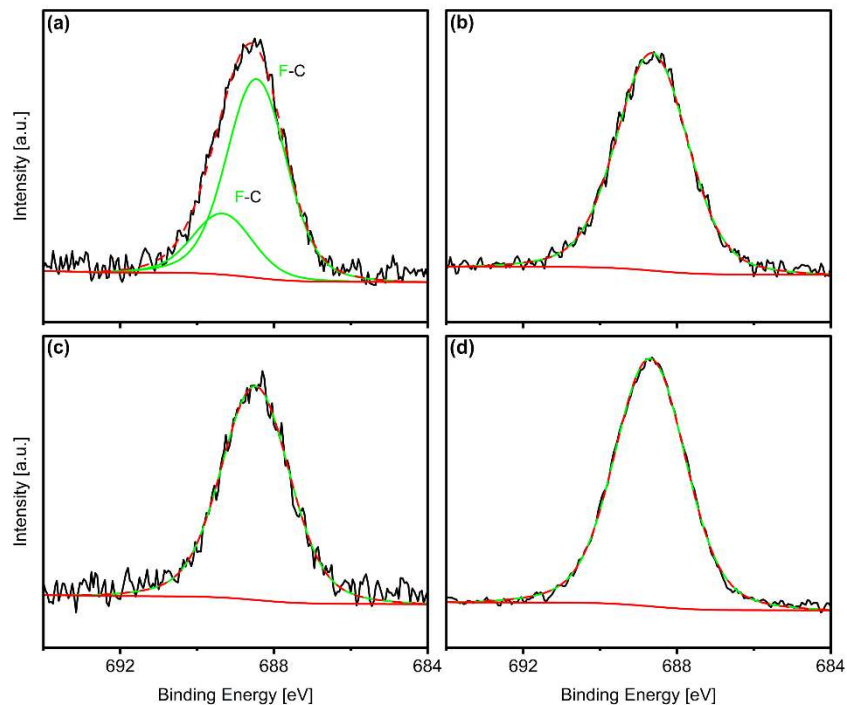


Figure S9. F 1s XPS spectra for as-made COF-LZU1 synthesized under (a) 0.02 eq. Sc(OTf)₃ and (b) 0.09 eq. Sc(OTf)₃, and as-made TAPB-PDA synthesized under (c) 0.02 eq. Sc(OTf)₃ and (d) 0.15 eq. Sc(OTf)₃.

Table S1. Analysis of XPS spectra for as-made COF-LZU1 synthesized under 15 eq. 10.5 M acetic acid, 0.02 eq. Sc(OTf)₃, and 0.09 eq. Sc(OTf)₃.

Catalytic condition	Element	Environment	Position [eV]	Atom %	Element %	Element % (from pristine COFs)
15 eq. 10.5 M acetic acid	C	C-C	284.5	39.78	84.02	84.02
		C-N	285.5	30.40		
		C-O	285.5	8.38		
		C=O	288	2.28		
		O-C-N	289	1.87		
		Oxidized Carbon	290.5	1.31		
		$\pi^* \leftarrow \pi$ shakeup	291.5	0		
	N	C=N=C	399	9.81	13.24	13.24
		C-NH ₂ , C ₂ -N-H	400	1.96		
		C-NH ₃ ⁺	401.5	0.21		
		Unknown state	404	1.26		
	O	C=O, C-O	533	1.67	2.74	2.74
		Unknown state	535	1.07		
0.02 eq. Sc(OTf) ₃	C	C-C	284.5	36.36	83.35	82.57
		C-N	285.5	29.28		
		C-O	286.5	9.56		
		C=O, C-F	287.5	2.88		
		O-C-N	289	1.85		
		Oxidized Carbon	290	1.46		
		$\pi^* \leftarrow \pi$ shakeup, CF ₂ , CF ₃	291	1.96		
	N	C=N=C	399	7.22	9.35	9.35
		C-NH ₂ , C ₂ -N-H	400	1.36		
		C-NH ₃ ⁺	401.5	0.29		
		Unknown state	402.5	0.48		
	O	C=O, C-O	532, 533.5	3.62	5.61	3.62
		S-O, S=O	535	1.99		
	Sc	Sc	404, 409	0.26	0.26	0
	S	SO _x	169, 170	0.32	0.50	0
		C-S	164, 165.5	0.18		
	F	C-F	688.5, 689	0.94	0.94	0
0.09 eq. Sc(OTf) ₃	C	C-C	284.5	46.48	72.25	70.75
		C-N	285.5	18.98		
		C=O, C-F	287.5	2.00		
		O-C-N	289	2.16		
		Oxidized Carbon	290.5	1.16		
		CF ₃	292.5	1.47		
	N	C=N=C	399	5.74	7.62	7.62
		C-NH ₂ , C ₂ -N-H	400	0.69		
		C-NH ₃ ⁺	401.5	0.60		
		Unknown state	403.5	0.59		
	O	C=O, C-O	532.5	10.27	11.75	10.27
		S-O, S=O	535	1.48		
	Sc	Sc	403, 408.5	0.50	0.50	0
	S	SO _x	169, 170	2.10	2.10	0
	F	C-F	688.5	5.77	5.77	0

Table S2. Analysis of XPS spectra for as-made TAPB-PDA synthesized under 15 eq. 10.5 M acetic acid, 0.02 eq. Sc(OTf)₃, and 0.15 eq. Sc(OTf)₃.

Catalytic condition	Element	Environment	Position [eV]	Atom %	Element %	Element % (from pristine COFs)
15 eq. 10.5 M acetic acid	C	C-C	284.5	48.68	88.02	88.02
		C-N	285.5	22.85		
		C-O	286.5	12.84		
		C=O	287.5	2.94		
		Oxidized Carbon	290.5	0.71		
	N	C=N=C	399	4.56	6.58	6.58
		C-NH ₂ , C ₂ -N-H	400	0.81		
		C-NH ₃ ⁺	401.5	0.28		
		Unknown state	402.5, 403.5	0.93		
	O	C=O, C-O	533	2.49	5.40	5.40
		Unknown state	535	2.91		
0.02 eq. Sc(OTf) ₃	C	C-C	284.5	52.26	87.24	86.31
		C-N	285.5	21.43		
		C-O	286.5	8.32		
		C=O, C-F	288	2.22		
		Oxidized Carbon	289.5	0.92		
		π* ← π breakup, CF ₂ , CF ₃	291	2.09		
	N	C=N=C	399	4.35	5.74	5.74
		C-NH ₂ , C ₂ -N-H	400	0.91		
		C-NH ₃ ⁺	401	0.23		
		Unknown state	402	0.25		
	O	C=O, C-O	532	3.29	5.37	3.29
		S-O, S=O	535	2.08		
	Sc	Sc	403, 409	0.31	0.31	0
	S	SO _x	169, 179	0.31	0.44	0
		C-S	164, 165.5	0.13		
	F	C-F	688.5	0.89	0.89	0
0.15 eq. Sc(OTf) ₃	C	C-C	284.5	34.91	78.21	76.38
		C-N	285.5	31.07		
		C-O	286.5	7.16		
		C=O, C-F	288.5	2.32		
		Oxidized Carbon	290	1.64		
		π* ← π breakup, CF ₂ , CF ₃	293	1.11		
	N	C=N=C	399	2.35	3.72	3.72
		C-NH ₂ , C ₂ -N-H	400	0.59		
		C-NH ₃ ⁺	402	0.14		
		Unknown state	403.5	0.64		
	O	C=O, C-O	532	8.18	12.62	8.18
		S-O, S=O	534	4.44		
	Sc	Sc	403, 408	0.61	0.61	0
	S	SO _x	169, 170	1.16	1.28	0
		C-S	164, 165.5	0.12		
	F	C-F	688.5	3.58	3.58	0

6. Crystallographic analysis of as-made COFs: Reaction time sensitivity, indexing, analysis and estimation of edge amine content

Reaction time sensitivity: Figure S10 compares the PXRD patterns for the 0.02 eq. $\text{Sc}(\text{OTf})_3$ -catalyzed COF-LZU1 and TAPB-PDA COFs after 1 h and 24 h synthesis. In the case of COF-LZU1, the highest crystallinity results from the 1 h reaction; increasing reaction time leads to attenuation of the characteristic reflections and a slight shift of the (100) peak to higher angles, the latter consistent with some loss of the eclipsed stacking. In the case of the TAPB-PDA COF, higher order crystallinity emerges with extended 24 h reaction, with the clear emergence of the (220), (320), and (330) reflections. The nominal reaction conditions of 1 h for COF-LZU1 and 24 h for TAPB-PDA correspond to the conditions leading to the most crystalline product.

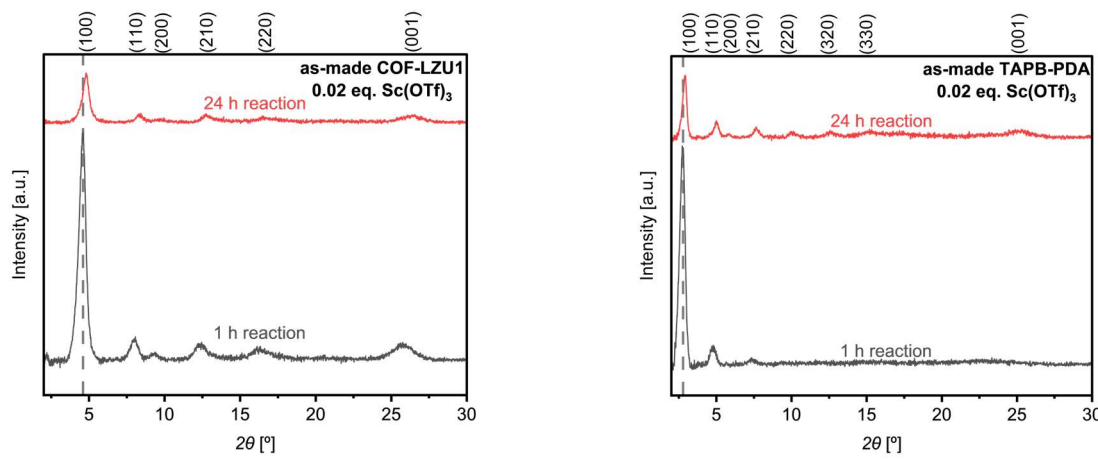


Figure S10. PXRD patterns of as-made COF-LZU1 and as-made TAPB-PDA synthesized under 1h and 24h reactions.

Crystallographic indexing: Lattice parameters are derived from the fitted crystal lattices after Pawley refinements with the pXRD patterns using Material Studio. (100) and (001) peak positions and full width at half maximum (FWHM) are derived from Gaussian fits for all peaks. Crystallite sizes are calculated from FWHM and peak positions using the Scherrer equation,

$$\Gamma = (K \times \lambda) / (\beta \times \cos\theta),$$

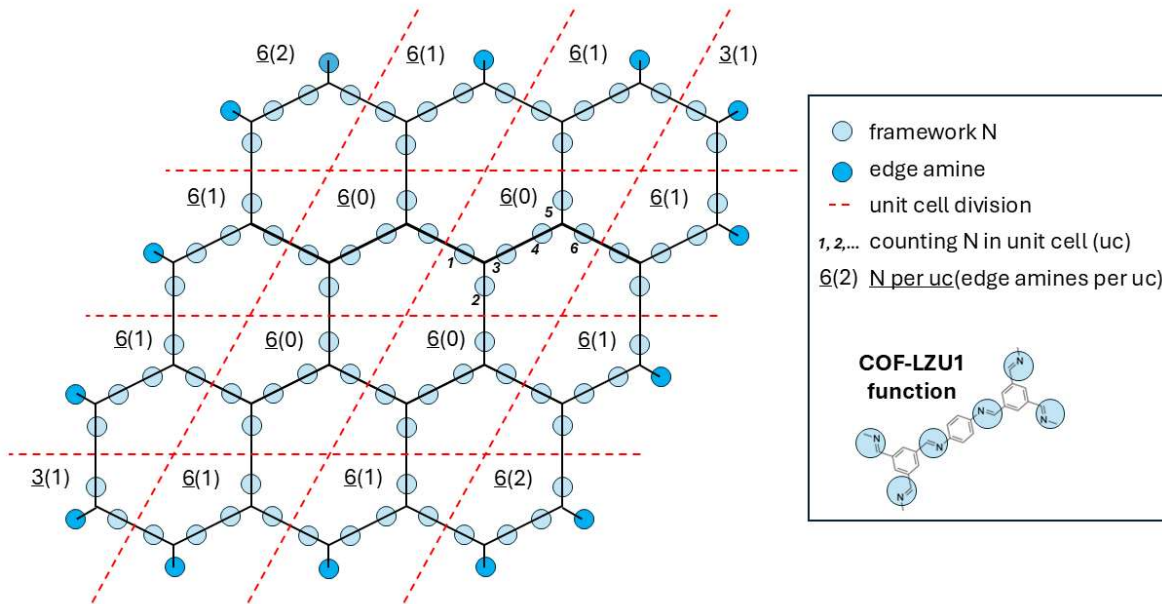
where Γ is the mean size of the crystalline domains, K (0.9) is the dimensionless shape factor, λ (1.5406 Å) is Cu K α wavelength, β is the FWHM in radians, and θ is the Bragg angle. In-plane and out-of-plane crystallite sizes are roughly estimated from (100) and (001) peaks, respectively.

Table S3. Peak positions, lattice parameters, FWHM, and calculated crystallite sizes derived from pXRD patterns of as-made COF-LZU1 and as-made TAPB-PDA synthesized under different catalytic conditions.

COFs	Catalytic condition	(100) peak position [°]	Lattice parameter (in-plane) [Å]	(100) peak FWHM [°]	Crystallite size (in-plane) [nm]	(001) peak position [°]	Lattice parameter (out-of-plane) [Å]	(001) peak FWHM [°]	Crystallite size (out-of-plane) [nm]
COF-LZU1	15 eq. 10.5 M acetic acid	4.86	a = 20.720 b = 21.307	0.59	14.04	26.27	c = 3.8	1.48	5.74
	35 eq. 10.5 M acetic acid	4.88	a = 20.923 b = 20.914	0.58	14.28	26.39	c = 3.8	1.30	6.54
	55 eq. 10.5 M acetic acid	4.85	a = 21.293 b = 20.948	0.62	13.36	26.36	c = 3.7	1.13	7.52
	0.02 eq. Sc(OTf) ₂	4.56	a = 22.042 b = 22.049	0.58	14.28	25.80	c = 3.7	1.67	5.08
	0.04 eq. Sc(OTf) ₂	4.54	a = 22.478 b = 22.075	0.60	13.80	25.98	c = 3.7	1.81	4.69
	0.09 eq. Sc(OTf) ₂	4.49	a = 22.465 b = 22.308	0.60	13.80	25.76	c = 3.7	1.60	5.30
	(eclipsed stacking from simulation)	4.63	a = b = 22.040	--	--	24 - 27	c = 3.7	--	--
TAPB-PDA	20 eq. 10.5 M acetic acid	2.94	a = 33.868 b = 37.501	0.37	22.37	25.20	c = 3.7	1.83	4.63
	35 eq. 10.5 M acetic acid	2.87	a = 35.721 b = 35.395	0.38	21.78	25.13	c = 3.3	1.57	5.40
	55 eq. 10.5 M acetic acid	2.91	a = 35.076 b = 37.718	0.36	22.99	25.24	c = 3.7	1.51	5.62
	0.02 eq. Sc(OTf) ₂	2.89	a = 37.897 b = 37.819	0.35	23.65	25.03	c = 3.6	2.35	3.61
	0.09 eq. Sc(OTf) ₂	2.74	a = 37.336 b = 37.220	0.42	19.71			--	
	(eclipsed stacking from simulation)	2.73	a = b = 37.467	--	--	24 - 27	c = 3.6	--	--

Estimation of terminal edge amines based on crystallite size for COF-LZU1

We estimate the maximum fraction of overall framework N associated with edge amines on the basis of XRD estimates of COF crystallite size and fitted lattice parameters (**Table S3**). **Scheme S1** depicts a 2D COF-LZU1 sheet comprised of a 3×3 array of hexagonal pores.



Scheme S1. Depiction of a 2D COF-LZU1 sheet comprised of a 3×3 array of hexagonal pores, with indication of positions and enumeration of framework N and edge amines per unit cell (uc).

Generally, for an (n pore) \times (n pore) array...

The total number of framework N, N_{tot} , is given by:

$$N_{tot} = [(n + 1) \cdot (n + 1) - 1] \cdot 6 = 6 \cdot (n^2 + 2n)$$

The total number of edge amines, N_{edge} , is given by:

$$N_{edge} = 4 \cdot (n - 1) + 6$$

Hence, for the schematized example above, where $n = 3$...

$$N_{tot} = 6 \cdot (3^2 + 2 \cdot 3) = 90$$

The total number of edge amines, N_{edge} , is given by:

$$N_{edge} = 4 \cdot (3 - 1) + 6 = 14$$

In the case of COF-LZU1...

XRD analysis (**Table S3**) suggests crystallites of ca. 14 nm and in-plane lattice dimensions of ca. 2.0 nm. Thus, $n \sim \frac{14}{2} = 7$. For COF-LZU1 crystallites comprised of 7 pore \times 7 pore COF sheets, the maximum fraction of overall framework N that are associated with edge amines can be estimated as

$$\frac{N_{edge}}{N_{tot}} = \frac{4 \cdot (n - 1) + 6}{6 \cdot (n^2 + 2n)} = \frac{4 \cdot (7 - 1) + 6}{6 \cdot (7^2 + 2 \cdot 7)} = \frac{30}{378} = 0.079 \sim 8\%$$

Hence, we estimate that a maximum of 8% of all framework N could be associated with edge amines without accounting for the fact that some of these would be formyl groups.

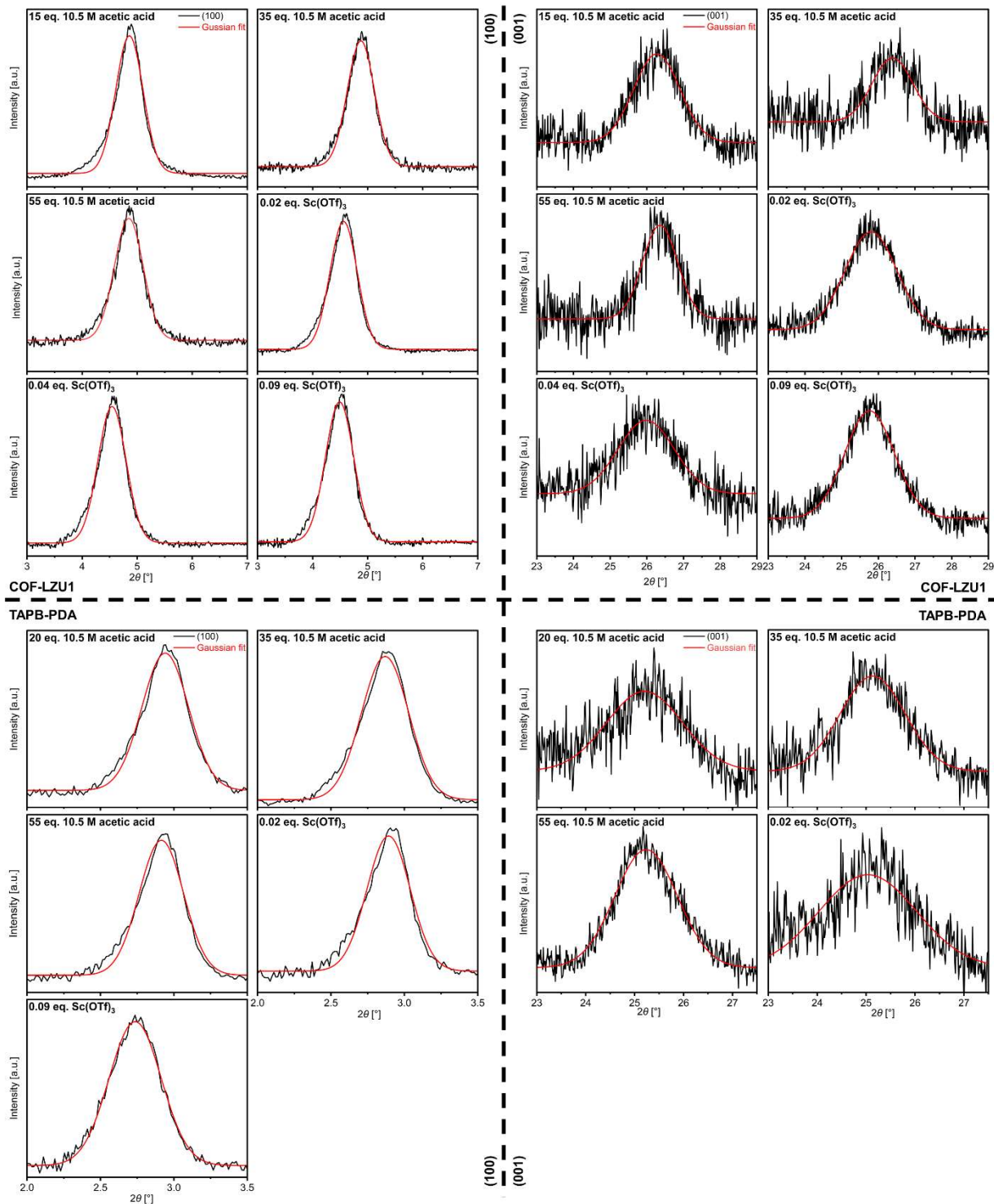


Figure S11. Gaussian fits of (100) and (001) pXRD peaks measured for as-made COF-LZU1 and TAPB-PDA synthesized under different catalytic conditions.

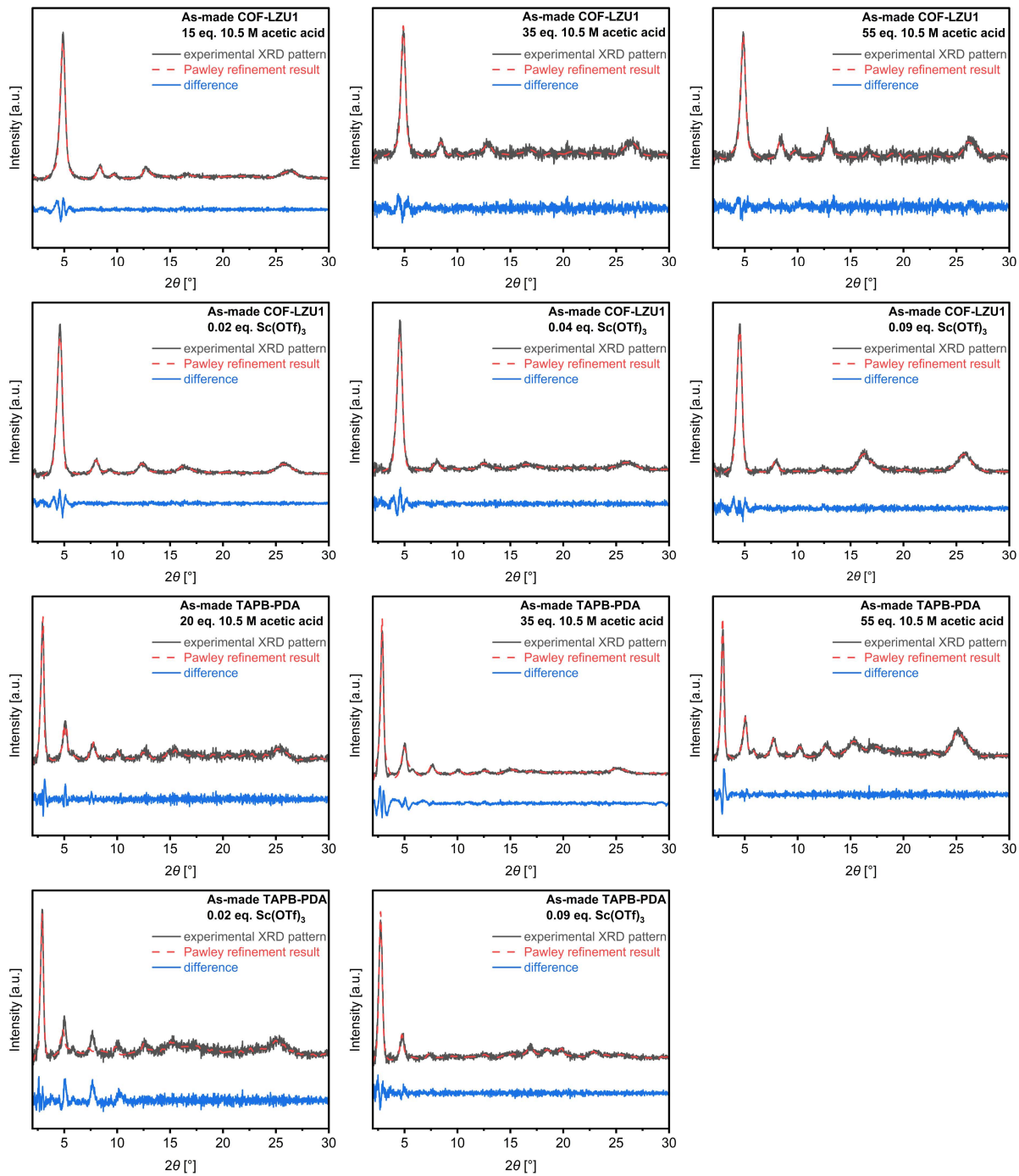


Figure S12. Pawley refinements of pXRD patterns measured for as-made COF-LZU1 and TAPB-PDA synthesized under different catalytic conditions.

7. DFT simulation of metal triflate binding to COF framework functionality as a function of metal

We have analyzed the relative binding strengths of two alternative and less efficient metal triflates found in Dichtel's work to yield semicrystalline ($\text{Yb}(\text{OTf})_3$) and nearly amorphous ($\text{Zn}(\text{OTf})_2$) 2D imine-based COFs.

Table S4. DFT simulation results of calculated binding energies with COF-LZU1 trilayers for various metal triflates (MTs) **(a)** coordinated with two defects resulting in an amine-MT-amine linkage and **(b)** adsorbed on an imine bond of the top layer of the pristine COF-LZU1.

Metal triflate (MT)	(a) [amine]—MT—[amine]	(b) [surface imine]—MT	$\Delta E_{(a)-(b)}$
$\text{Sc}(\text{OTf})_3$	-222 kJ/mol	-101 kJ/mol	-121 kJ/mol
$\text{Yb}(\text{OTf})_3$	-242 kJ/mol	-126 kJ/mol	-116 kJ/mol
$\text{Zn}(\text{OTf})_2$	-286 kJ/mol	-164 kJ/mol	-122 kJ/mol

8. Evolution of the morphology, composition, and crystallinity of as-made COF-LZU1 under 0.02 eq. $\text{Sc}(\text{OTf})_3$ with different amounts of DI water

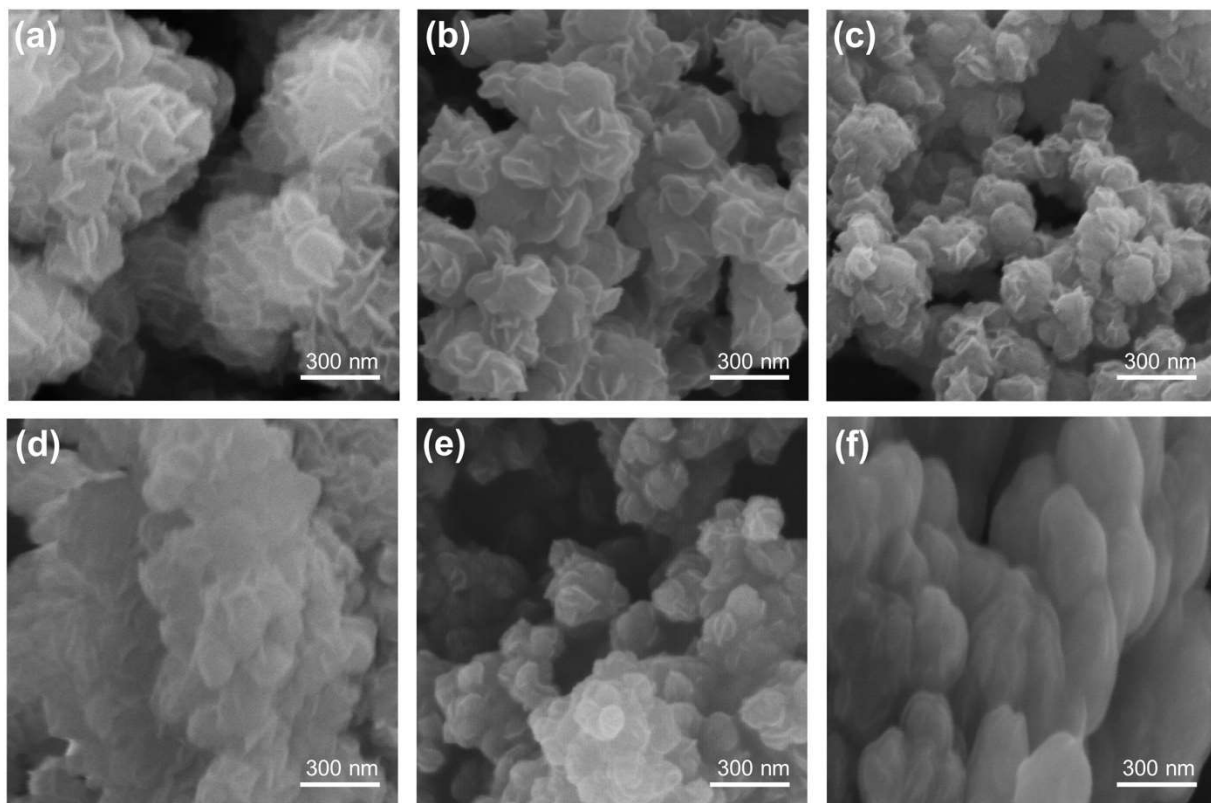


Figure S13. SEM images of as-made COF-LZU1 synthesized with 0.02 eq. $\text{Sc}(\text{OTf})_3$ and **(a)** 0 eq., **(b)** 5 eq., **(c)** 10 eq., **(d)** 20 eq., **(e)** 35 eq., and **(f)** 60 eq. of DI water.

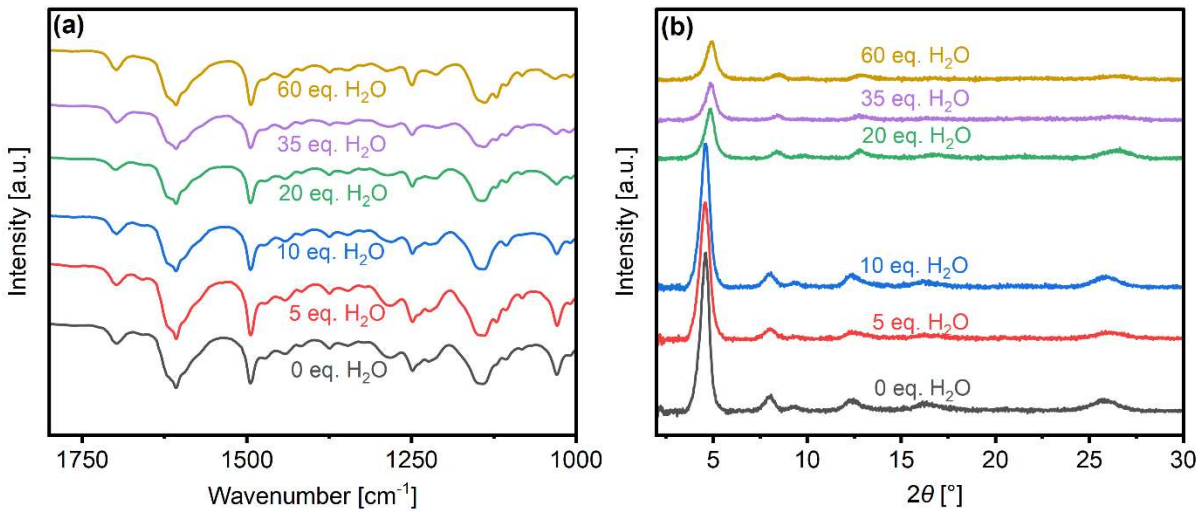


Figure S14. (a) FTIR spectra and (b) pXRD patterns of as-made COF-LZU1 synthesized with 0.02 eq. $\text{Sc}(\text{OTf})_3$ and the specified amounts of DI water.

9. COF-LZU morphology upon activation

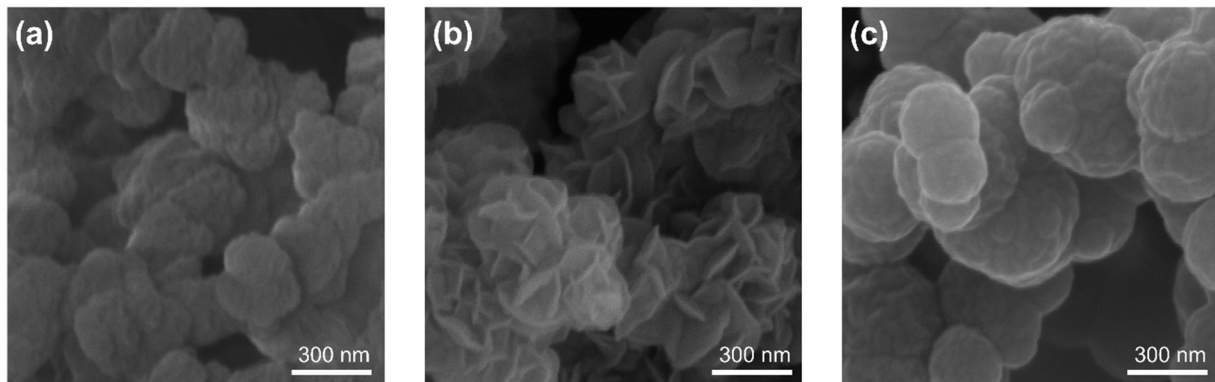


Figure S15. SEM images of activated COF-LZU1 synthesized under (a) 15 eq. 10.5 M acetic acid, (b) 0.02 eq. $\text{Sc}(\text{OTf})_3$, and (c) 0.09 eq. $\text{Sc}(\text{OTf})_3$.

10. Theoretical pore size changes with defect introduction

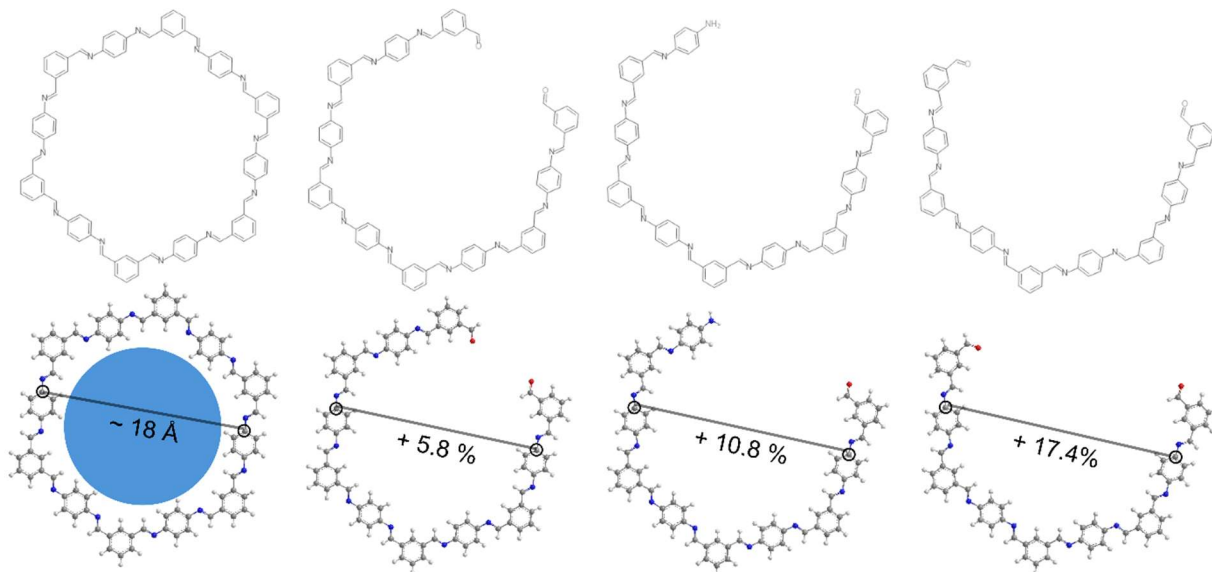


Figure S16. Molecular structures of the pore of COF-LZU1 upon introduction defects and ‘indicated’ pore sizes simulated using 3D Chem.

11. Hierarchical COF Literature comparison

Table S5. Comparison of synthetic conditions and texture of hierarchical COF-LZU1

COF	Hierarchical structuring method	Synthesis		Post processing	BET surface area and % change by structuring	Ref.
		T [°C]	Time [h]			
Tp-Bpy	Sacrificial templating w/ polystyrene spheres	80 °C	24 h	Hot water wash; THF Soxhlet extraction	723 m ² /g (+23 %)	4
COF-TPDA-BPDA	Sacrificial templating w/ pre-made 50 nm SiO ₂ nanoparticles	120 °C	72 h	Solvent wash, 1M NaOH treatment	742 m ² /g	5
COF-TpPa	<i>In-situ</i> templating	Freeze dry, then 90 °C	5 h (freeze dry), 12 h (oven heat)	Hot water wash	579 m ² /g	6
TAPA-TFPA	Adding growth modifier	25 °C	72 h	Solvent wash	1453 m ² /g	7
CX4-BD	Controlling monomer concentration	25 °C	72 h	EtOH Soxhlet extraction	N/A	8
TB-G-COF TB-H-COF	Synthesis temperature programming	80, 120, 150 °C	4 - 360 h	MeOH wash, scCO ₂	1598 m ² /g (+118 %)	9
COF-LZU1 rosette	Controlling catalyst concentration	25 °C	1 h	Solvent wash, water activation	876 m ² /g (+286 %)	This work

12. RdB and MB adsorption equilibration times

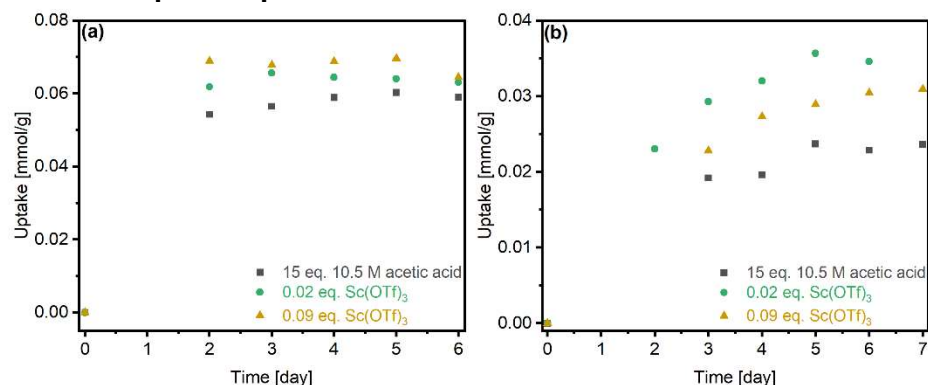


Figure S17. (a) RdB (b) MB adsorbed onto activated COF-LZU1 powders as a function of time.

13. References

- (1) Artemenko, A.; Shchukarev, A.; Štenclová, P.; Wagberg, T.; Segervald, J.; Jia, X.; Kromka, A. Reference XPS Spectra of Amino Acids. In *IOP Conference Series: Materials Science and Engineering*; IOP Publishing Ltd, 2021; Vol. 1050. <https://doi.org/10.1088/1757-899X/1050/1/012001>.
- (2) Chen, C.; Levitin, G.; Hess, D. W.; Fuller, T. F. XPS Investigation of Nafion® Membrane Degradation. *J Power Sources* **2007**, *169* (2), 288–295. <https://doi.org/10.1016/j.jpowsour.2007.03.037>.
- (3) Wang, L.; Xu, H.; Qiu, Y.; Liu, X.; Huang, W.; Yan, N.; Qu, Z. Utilization of Ag Nanoparticles Anchored in Covalent Organic Frameworks for Mercury Removal from Acidic Waste Water. *J Hazard Mater* **2020**, *389*. <https://doi.org/10.1016/j.jhazmat.2019.121824>.
- (4) Zhao, X.; Pachfule, P.; Li, S.; Langenhahn, T.; Ye, M.; Schlesiger, C.; Praetz, S.; Schmidt, J.; Thomas, A. Macro/Microporous Covalent Organic Frameworks for Efficient Electrocatalysis. *J Am Chem Soc* **2019**, *141* (16), 6623–6630. <https://doi.org/10.1021/jacs.9b01226>.
- (5) Li, W.; Jiang, H. X.; Cui, M. F.; Wang, R.; Tang, A. N.; Kong, D. M. SiO₂ Templates-Derived Hierarchical Porous COFs Sample Pretreatment Tool for Non-Targeted Analysis of Chemicals in Foods. *J Hazard Mater* **2022**, *432*. <https://doi.org/10.1016/j.jhazmat.2022.128705>.
- (6) Karak, S.; Dey, K.; Torris, A.; Halder, A.; Bera, S.; Kanheerampockil, F.; Banerjee, R. Inducing Disorder in Order: Hierarchically Porous Covalent Organic Framework Nanostructures for Rapid Removal of Persistent Organic Pollutants. *J Am Chem Soc* **2019**, *141* (18), 7572–7581. <https://doi.org/10.1021/jacs.9b02706>.
- (7) Wang, S.; Yang, Y.; Zhang, H.; Zhang, Z.; Zhang, C.; Huang, X.; Kozawa, D.; Liu, P.; Li, B. G.; Wang, W. J. Toward Covalent Organic Framework Metastructures. *J Am Chem Soc* **2021**, *143* (13), 5003–5010. <https://doi.org/10.1021/jacs.0c13090>.
- (8) Garai, B.; Shetty, D.; Skorjanc, T.; Gándara, F.; Naleem, N.; Varghese, S.; Sharma, S. K.; Baias, M.; Jagannathan, R.; Olson, M. A.; Kirmizialtin, S.; Trabolsi, A. Taming the Topology of Calix[4]Arene-Based 2D-Covalent Organic Frameworks: Interpenetrated vs Noninterpenetrated Frameworks and Their Selective Removal of Cationic Dyes. *J Am Chem Soc* **2021**, *143* (9), 3407–3415. <https://doi.org/10.1021/jacs.0c12125>.

- (9) Mu, Z.; Zhu, Y.; Zhang, Y.; Dong, A.; Xing, C.; Niu, Z.; Wang, B.; Feng, X. Hierarchical Microtubular Covalent Organic Frameworks Achieved by COF-to-COF Transformation. *Angewandte Chemie - International Edition* **2023**, *62* (17). <https://doi.org/10.1002/anie.202300373>.